Erosion Corrosion Evaluation of CrN/AlN Multilayer Coatings, by Varying the Velocity and Impact Angle of the Particle

W. Aperador[*]*, J. Caballero-Gómez, A. Delgado*

Departament of Engineering, Universidad Militar Nueva Granada, Carrera 11 No. 101-80, Fax:+57(1) 6343200, Bogotá, Colombia.
[*]E-mail: g.ing.materiales@gmail.com

In order to provide solutions to erosion corrosion in industrial devices, thin films of CrN/AlN were deposited on AISI D3 steel substrates using a magnetron sputtering system multitarget with rf (13.56 MHz), from Al and Cr targets of high purity (99.99%) in an atmosphere composed by Ar/N_2. The erosion tests and corrosion erosion were made by equipment which lets the change of the impact angle and the jet velocity of the silica particle; moreover the equipment is engaged with a potentiostat. The polarization curves were done in the resting potential. Subsequently of the realization of the polarization curves experiments, the samples were analyzed by scanning electron microscopy. The coating performance is compared with the AISI D3 steel without coating. The degradation mechanisms for PVD coating and uncoated steels have been presented with the help of diagrams wear mechanism.

1. INTRODUCTION

The superficial modification of different devices by thin films or hard coatings deposition is a process using widely to protect ceramic and metallic materials against phenomenons such as wear, fatigue, corrosion and many others which involve the deterioration of the surface. In this regard, the modern methods that implied techniques of physical vapor deposition by plasma assisted offer a superior grade of control in the films obtention with a stoichiometry and specific microstructure, leading to coatings with unique properties [1]. Different types of coatings have been obtained with the purpose of increase the corrosion resistance in metallic elements used in corrosive atmospheres. To achieve this, hard coatings such as AlN aluminum nitride whose good properties of thermal conductivity of 320 W m^{-1} K^{-1} and thermal expansion coefficient of 5.3 x 10-6 K^{-1} close to that of

silicon have attracted considerable interest to research of this material in the recent years, being applied in an industry as demanding as it is microelectronics owing to its thermal resistance and anticorrosion properties [2-5]. Other of the materials used to mitigate superficial damage is the CrN chromium nitride, due to its excellent mechanical properties (Hardness around 20GPa), tribological (friction coefficient comparable with the TiN when is in contact with the steel), high chemical and thermal stability with a oxidation temperature around 700° C which make the coating useful in a wide variety of industrial applications such as the automotive industry [6-8]. Nevertheless, despite of the excellent exhibited properties by both coatings, the corrosion resistance of these materials has been conditioned by the presence of inherent structural defects such as micropores, valleys and cracks that appear during deposition hence the focused effort by researchers in the optimization of the deposition parameters. The presence of these defects is an important factor to taking into account since influence the coating integrity, not only in corrosion resistance terms also in tribological and mechanical properties [2-7].

The erosion wear, understood as the provoked damage by the impact of hard particles present in a fluid, it affects equipments such as turbines, pumps, pipes and other devices that transport fluids, which can be subjected to pressure shocks provoking effects like erosion of solid surfaces, vibrations, excessive noises, decreased efficiency and others. This finally results in huge costs for repair or replacement of these types of equipments [9]. In addition, the pieces that are exposed to the action of these fluids can be present a corrosion process by erosion, which rapidly decreasing its service life. The corrosion by erosion is acceleration in the corrosion velocity of a metal due to the relative movement of a corrosive fluid and the metal surface [10], furthermore, if the fluid presents hard particles content in suspension, it has to increase the erosion effect that cause the metal wear. Currently, the hard coatings such as the nitrates based on transition metals deposited using techniques like physical vapor deposition and over different steel substrates, have been converted in the solution of many engineering problems and among them the corrosion caused by chemical inertness [11, 12].

The aim of this work, is study the performance of the wear mechanisms in multilayer coatings type [CrN/AlN]$_{50}$, which offer protection for the industrial use substrate such as the AISI D3 steel. With the purpose of analyse its response with the variation of the velocity and the impact angle. This study allows collecting enough information to the obtainment of wear diagrams that indicate the type of predominant wear in the coatings.

2. EROSION MODEL

In the erosion-corrosion studies the effect caused by the impact angle is normally ignore, despite this has a significant effect on the erosion rate [13]. In this work is considerate a model that estimates the erosion rate for ceramic materials, a brief description is made for this model.

2.1 Erosion rate

The erosion rate of a ceramic surface can be expressed as the product of the characteristic erosion rate $(ER)_c$ by the dimensionless function of the local erosion rate $\bar{E}_{lim}$ [14, 15]. The

characteristic erosion rate is given in an environment where all the particles have a mean size and impact the ceramic target with a normal incidence. [16]

$$(ER)_c \equiv \varepsilon_p(U, 0, \bar{v}_{p.\infty}) \cdot (\bar{v}_p N_p U)_\infty \tag{1}$$

Where ε_p is the specific erosion yield evaluated at a flow velocity U, at a normal incidence angle, an abrasive particle volume $\bar{v}_{p\cdot\infty}$, and $(\bar{v}_p N_p)_\infty$ is the volume fraction of the principal current. [16]

$$\varepsilon_p(U, 0, \bar{d}_{p.\infty}) = \varepsilon_{p.ref.}(V_p/V_{p.ref.})^n \cdot \cos(\theta_i)^m \cdot (d_p/d_{p.ref.})^{3 \times l} \tag{2}$$

The $\varepsilon_{p.ref.}$ is the value of ε_p evaluated at a fluid velocity $V_p = 16\ ms^{-1}$, at an impact angle $\theta_i = 60°$ and a particle volume v_p corresponding to a particle diameter $d_p = 250\ \mu m$. The erosion parameters l, m, n are dimensionless exponents which describe the sensitivity of the erosion yield to the particle size, the incidence angle and the fluid velocity respectively. Finally the erosion rate is calculated by multiplying the $(ER)_c$ by the $E_{lim} = \cos\theta^{m+1}$ and by the following power series representing the average erosion rate. [16-20]

$$\bar{E}_{lim} \approx (2/\pi) + [(11/16) - (8/(3\pi))] \cdot m + [(2/(3\pi)) - (3/16)] \cdot m^2 \tag{3}$$

3. EXPERIMENTAL DETAILS

[CrN/AlN]$_{50}$ multilayers were deposited over the AISI D3 steel substrates (diameter 2 cm; thickness 4mm) and Si (orientation 100; 1.7 cm of side; 280 microns of thickness), which were cleaned by ultrasound in a sequence of 15 minutes in a ethanol and acetone bath. The coatings were obtained by means of the magnetron sputtering multi-target in r.f technique (13.56 MHz). For the deposition of the coatings were used Cr and Al targets of 4 inches of diameter with a purity of 99.9%. The base interior pressure of the vacuum chamber was 7.0×10^{-6} mbar. Before starting the deposition for the subtrates were subjected to a cleaning by plasma during 20 minutes in Ar atmosphere of -400V in r.f. During the growth, the working gases were a mixture of Ar (93%) and N$_2$ (7%) with a total working pressure of 6×10^{-3} mbar at a substrate temperature of 300 °C and a substrate bias rf -50V and an output of 400W. For the deposition of the multilayer the aluminum target, as the chromium was covered periodically by the shutter in alternately form, while the substrate was kept under circular rotation in front of the targets to facilitate the formation of the coatings.

With the purpose of study the influence of the synergy between dynamic corrosion, erosion and erosion corrosion of multilayers coatings, were deposited [CrN/AlN]$_{50}$ systems controlling the opening and closing times of the shutter. The thickness of the coating was obtained by a DEKTAK 8000 profilometer with a peak diameter of 12±0.04 μm at a scanning length between 1000 μm – 1200 μm. For the 50 bilayers sample, the thickness was 3.00 ± 0.04 μm and given that the coatings were obtained under the same growth parameters and total time deposit (3 hours), is possible to state that the multilayers systems have a thickness around of this value.

Regarding the evaluation of the erosion corrosion resistance was used an equipment of particle impinging jet, as is shown in the figure 1. It consists in a particle jet in an aqueous flow that is keeping in constant movement by a recirculation system consisting of hoses, couplings and a magnetic drive pump which controls the flow velocity, the fluid temperature is regulated using a thermal resistance. The acrylic chamber allows having the adequate conditions for carrying out the tests by direct attack or by immersion and the impact angle is selected by means of the specimen holder position. The equipment allows controlling three independences variables which are the fluid temperature, the flow velocity and the impact angle. The tests were performed varying the impact angle at 30°, 60° and 90°, the fluid velocity of the particle V1=14.2 ms^{-1} and V2=18.5 ms^{-1}.
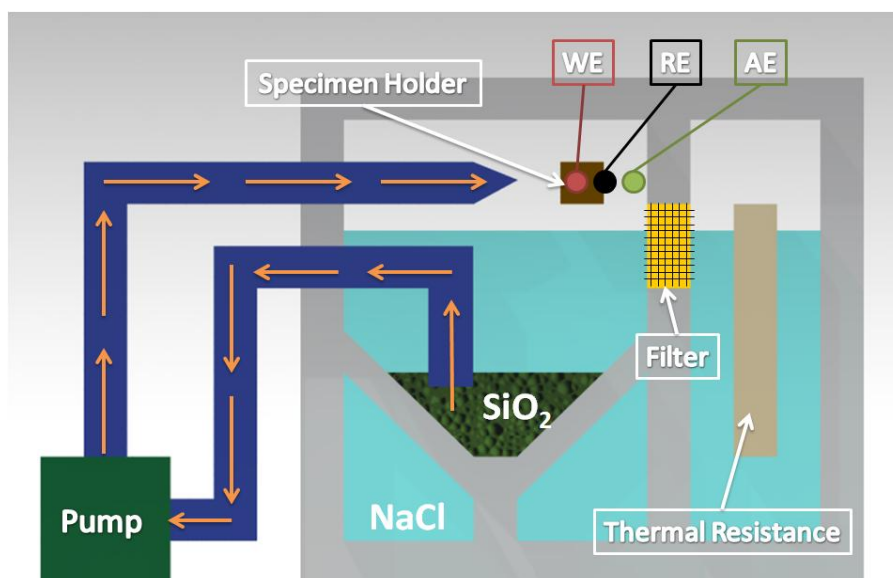
Figure 1. Scheme of the equipment used in the erosion-corrosion wear test, AE: Auxiliary electrode, WE: Working electrode, RE: Reference electrode.

The electrochemical cell is composed by an auxiliary electrode (graphite), a reference electrode (Ag/AgCl) contained in a Luggin capillary which permits determining in an accurate way the potential between the reference electrode and the working electrode which for the purposes of tests were used AISI D3 steel coated. The figure 2 shows the disposition of the electrodes the system. For the dynamic corrosion and erosion-corrosion evaluations were used a Gamry PCI-4 model potentiostat – galvanostat by means of the Tafel potentiodynamic curves technique. The specimens were situated under immersion in a NaCl 0.5 M prepared with distilled water and (SiO_2) silica particles which have a size between 210 μm y 300 μm under a proportion of 20 wt% with respect to the medium. The Tafel diagrams were obtained in a dynamic form at a scanning velocity of 0.5 mV/s en a voltage range of -0.25V a 0.55V using an exposed area of 1cm^2, the electrochemical behavior was evaluated subsequently at 45 minutes, necessary time for the stabilization of the open circuit potential. The standards used in metrics and calculations correspond to the G5 and G59 ASTM [21, 22]. The

specimens were subjected to erosion wear during a total time of 240 minutes of exposure (duration of the tests by Tafel) at a 25°C of temperature.
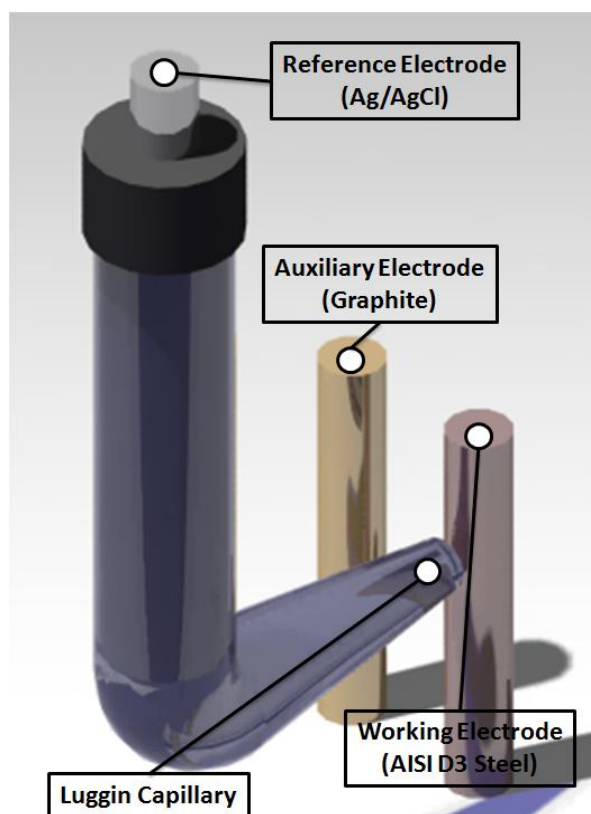

Figure 2. Scheme of the disposition of the electrodes in the system

During the immersion test in a NaCl 0.5 M solution with a presence of (SiO_2) silica particles. The specimens were removed from the solution in a certain interval of time (15 minutes), were cleaned with a water jet, were dried with hot air, and were weighed using a balance accurate to 0.1 mg; with the purpose of determinate the weight loss owing to the erosion. The microstuctural observation was performed using a high resolution scanning electron microscope, which has an energy dispersive spectroscopy system (EDX system); the SEM has a resolution of 1 nm at 30 kV.

4. RESULTS AND DISCUSSION

4.1 Estimation of the erosion rate

The erosion rate was estimated using the model mentioned above [14-20]. As a result, the necessary data were obtained to plot the erosion rate of the CrN/AlN multilayer coatings in function of the impact angle, to observe its behavior against the erosive wear as is shown in the figure 3.
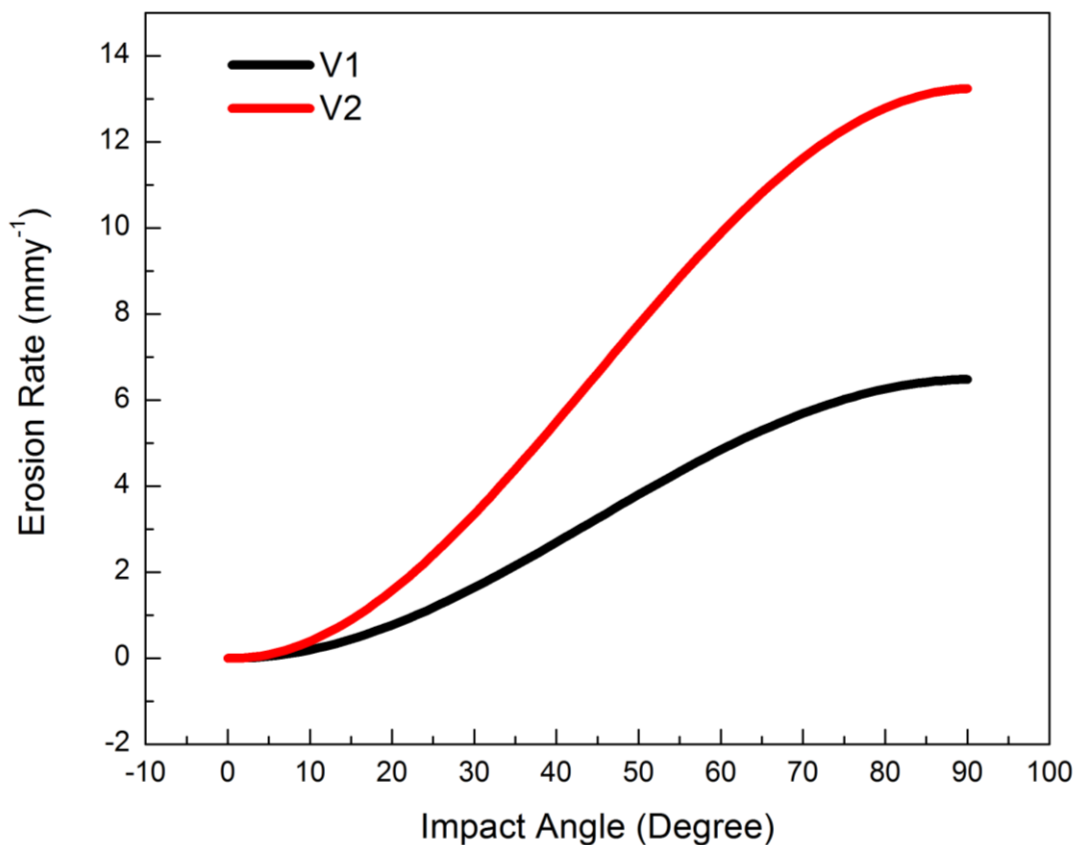
Figure 3. Erosion diagram: erosion rate at V1=14.2 ms^{-1} and V2=18.5 ms^{-1} in function of the impact angle.

The following data were taken of the tests performed to the implementation of the estimation model:

- Particle diameter: 210-300 µm (average 255 µm).
- Fluid velocity: 14.2 ms^{-1} and 18.5 ms^{-1}.
- Particle loading: 1ppm.
- Slurry density: 21.61 kgm^{-3}.
- Impact angles: 30°, 60° y 90°.

As regards the erosion parameters, the dimensionless exponent used were l=1; m=0.9; n=1.7; and $\varepsilon_{p,ref.}$=4.8E-3. In the table 1 shows the erosion rate estimation in mmy^{-1} with the model at impact angles of 30°, 60° and 90° degrees at velocities of 14.2 ms^{-1} and 18.5 ms^{-1}.

Table 1. Comparison of the rate of erosion at different angles and velocities

Erosion Rate	Impact Angle		
Velocity	30°	60°	90°
V1	1.54 mmy^{-1}	4.74 mmy^{-1}	6.48 mmy^{-1}
V2	3.15 mmy^{-1}	9.68 mmy^{-1}	13.24 mmy^{-1}

The wear at 90 degrees can be seen as 100% of the wear that can suffer the coating by erosion, taking into account that the highest wear occur when the impact angle is normal. The above allows observing how the erosive wear decreases respect to the impact angle diminution.

Table 2. Erosion in percentage

Erosion Rate	Impact Angle		
Velocity	30°	60°	90°
V1	23.78%	73.13%	100%
V2	23.78%	73.13%	100%

Observing the table 2 is obtained that the wear decreases to 26.87% an 76.22% when the impact angle is 60° and 30° respectively, independently of the fluid velocity in spite of this increases.

In addition, the model was proved comparing the submitted erosion rates by the model with experimental data from other study, which evaluated CrN and TiN coatings against the erosive effect [23]. The error percentage was 11.36% and 10.47% for the TiN and CrN respectively; it leads to an average error of 10.91% which is low to these kinds of systems.

4.2 Potentiodynamic sweep measurements

In the figure 4, shows the anodic polarization curves of the tested multilayers by dynamic corrosion, highlighting that the corrosion potentials in the CrN/AlN multilayers are moved into anodic zones (protection), when the angle and velocity of the fluid have been decreased, therefore, can be established a bidimensional distribution of the influence of the increased angle and velocity. (Table 3).

The obtained curves in the figure 4 generate an active corrosion behavior in the anodic zone, being more prominent for the multilayer with an impact angle of 90° and a linear velocity of 18.5 ms^{-2}. The multilayers generate zone of less electro-dissolution respect to the beginning of the electro-dissolution (250mV vs Ecorr), subsequently the active corrosion zone of the multilayers increases due to the increased corrosion density. The multilayers in a 0.5M NaCl medium presents a behavior change in the anodic branch, is can be distinguish as the beginning of the formation of general corrosion in stable form owing to higher increased of the corrosion density, indicating the regeneration of a corrosion products layer which allows stabilizing the current density around of this potential and prevents the increased of the dissolution velocity of the metal. This characteristic can be appreciated for all the potentiodynamics curves groups. In the table 3 is observed the decreased in the corrosion current velocity and density in multilayers coatings of CrN/AlN, when are evaluated at low fluid velocities and decreased of impact angle. This decreased can be attributed to the nature of the multilayer type structures, since the increased the number of multilayers increases the number of interfaces. The interfaces are zones where are presented structural disorders, they generate a change in

the crystallographic orientation, acting as dispersion points which difficulty the Cl ion migration from the surface to the metallic substrate and delay the beginning of the corrosive process. It leads to the required energy by the ions of the solution to migrate freely from the surface to the film/substrate interface is higher with the decreased of the impact angle and the fluid velocity. This behavior is reflected in the decreased of the current density and the corrosion velocity (table 3).
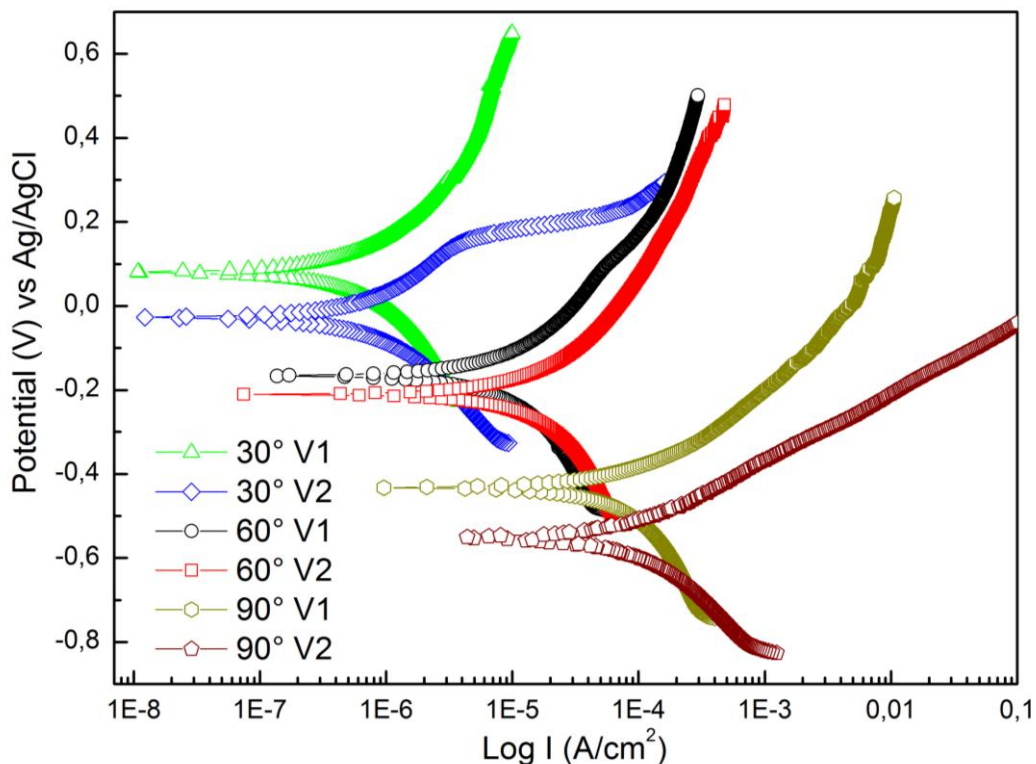
**Figure 4.** Polarization curves of the dynamic corrosion in a solution of 0.5 M NaCl.

Table 3. Parameter values obtained by electrochemical polarization curves for the multilayer.

Angle (Degree)	Velocity (ms^{-1})	Ecorr (V) vs Ag/AgCl	Icorr ($\mu A/cm^2$)	Vcorr×10^{-3} (μmy)
30°	V1	-0.125	0.431	0.62
	V2	-0.155	0.964	1.35
60°	V1	-0.313	2.13	3.00
	V2	-0.362	6.98	9.84
90°	V1	-0.507	10.3	14.52
	V2	-0.633	22.8	32.14

In the figure 5 compares the behavior of the different CrN/AlN multilayers, in the erosion corrosion system for the studied materials. The corrosion velocity as corrosion densities decreases in function of the decreasing of the impact angle and fluid velocity. Furthermore, it can be observed a generalized corrosion phenomenon in all of the multilayers, however the difference of the corrosion

velocity values is due to reaction kinetic depends on the tested angle, in as much as it dissolves with higher velocities for the 60° and 90° angles. In quantitative form is possible to group the Tafel polarization curves, being the curves of the coated steel with the multilayers and evaluated at angles of 60° and 90°, similar between them, these multilayers show a material dissolution in a moderate way, this phenomenon is found in those coatings, indicating the corrosion products regeneration which allow stabilizing the current density around this potential and prevent the increased of the dissolution velocity of the metal. For the polarization curves evaluated at 30° is obtained that from 315 mV vs. Ag/AgCl and 498 mV vs. Ag/AgCl, for the velocities of 18.5 m s^{-2} and 14.2 m s^{-2} respectively, the kinetic process is dominated by diffusion, which is the reason why the shape of the curves is modified.
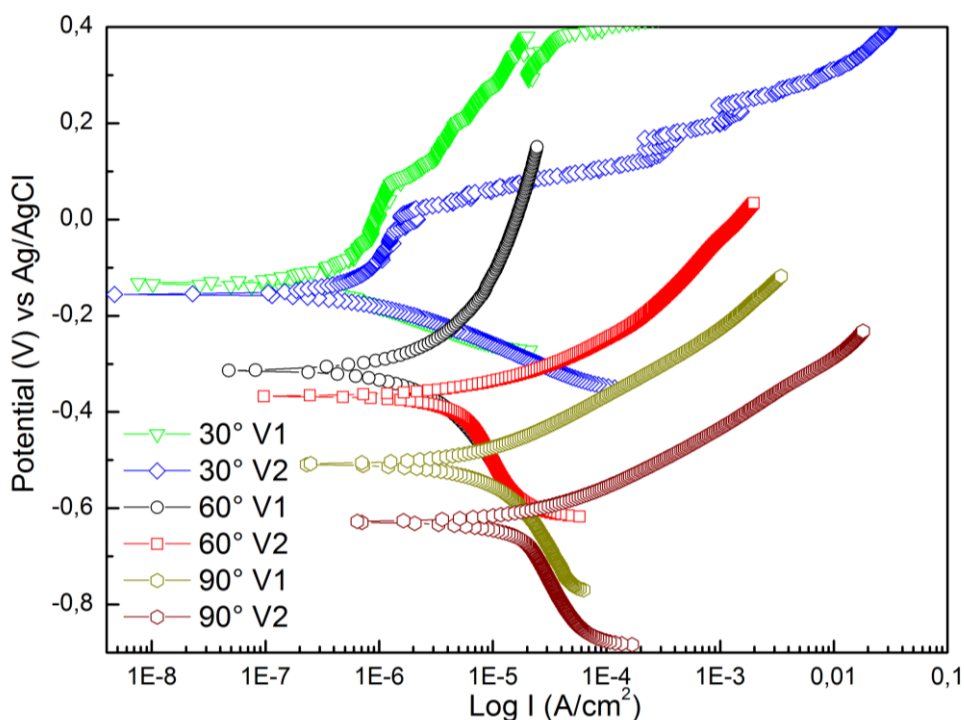
Figure 5. Polarization curves of erosion corrosion of the multilayer [CrN/AlN]$_{50}$ in 0.5M NaCl solution.

Table 4. Electrochemical parameters obtained from polarization curves in erosion corrosion system for the substrate and the multilayer [CrN/AlN]$_{50}$.

Angle (Degree)	Velocity (ms^{-1})	Ecorr (V) vs Ag/AgCl	Icorr (μA/cm^2)	Vcorr$\times10^{-3}$ (μmy)
30°	V1	0.0768	0.608	0.857
	V2	-0.0238	1.057	1.49
60°	V1	-0.161	8,41	11.84
	V2	-0.211	18.0	25.38
90°	V1	-0.433	102	143.82
	V2	-0.554	221	311.61

The registered data in the table 4 indicate, effectively, a less electrochemical performance than the dynamic corrosion (figure 4 and table 3) against the erosion corrosion, which shows a decreased of corrosion potentials and densities for the multilayers. All in all, the data (table 3) show a good behavior for the analyzed coatings at the angles of 30° in comparison with the 60° and 90° angles, when are subjected to a corrosive phenomenons. However, when are subjected to the erosive-corrosive, (table 4) the passive film normally formed on the surface is eliminated and removed by the action of hard particles leading to loss of the anticorrosive protection. On the other hand, the corrosion reduces the resistance of these coatings on the surface and favoring the improvement of increased of corrosion velocity in comparison with the dynamic corrosion (figure 4).

In other study, was observed that steel coated with CrN/AlN has corrosion potentials more electropositive compared to the uncoated steel AISI D3; this confirms the protective effects of the coatings [24]. Moreover the coatings generate a displacement of the curves towards lower values of the current density and potentials more noble than AISI D3 steel substrate which is related with the high interface number with nanometric bilayer, improving the response against the erosive and corrosive effect [25, 26]. Consequently, the results showed in the present work are in agree with J.C Caicedo et al [27]; that previously presented a research on the behavior of some steels and CrN/AlN coatings against erosion corrosion effect.

4.3 SEM scanning electron microscopy

The CrN/AlN multilayer coating evaluated at 30° was observed using microscopy to determinate the lowest suffered damage by the corrosive effect, and the synergetic effect of the erosion corrosion. In the figure 6a, is observed that the corrosive effect have not been generated an elevated wear, since the coating does not evidence some corrosion type. The fluid velocity effect (increased) is showed in the figure 6b, which indicates an initial wear by the general corrosion fractions observed in the micrograph; this effect is the same that was evidenced in the polarization curves, where the corrosion velocity increases when the fluid velocity increases.


(a)   (b)

(c)   (d)
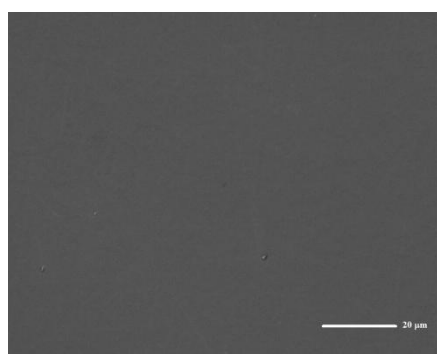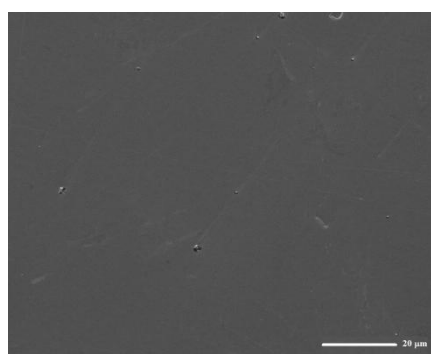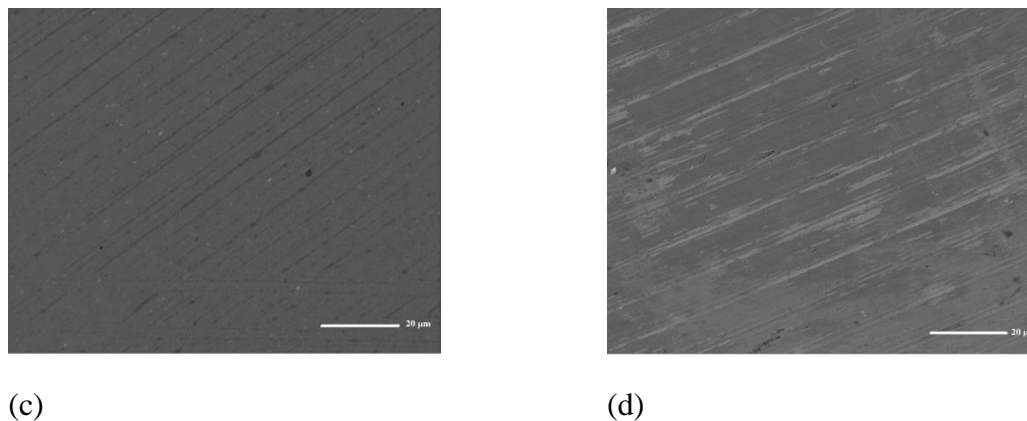
Figure 6. SEM micrographs for samples with degradation a) multilayer CrN/AlN for samples subjected to corrosion 30 ° and velocity 14.2 ms^{-2}, b) multilayer CrN/AlN for samples subjected to corrosion angle 30 ° and velocity 18.5 ms^{-2}, c) multilayer CrN/AlN for samples subjected to corrosion erosion angle 30 ° and velocity 14.2 ms^{-2}, d) multilayer CrN/AlN for samples subjected to corrosion erosion angle 30 ° and velocity 18.5 ms^{-2}.

In the figure 6c, is showed the wear produced by the impact energy of the abrasive silica particles at an angle of 30°, this type of wear is generated by the particles abrasion, in the figure 6d, is observed a higher wear due to a deep grooves observed over all the surface, in as much as the particles generates a continuous damage and increases in comparison with the figure 6c by the velocity change, additionally, the corrosive effect generates the dissolution of corrosion action.

4.4 Synergy between erosion corrosion
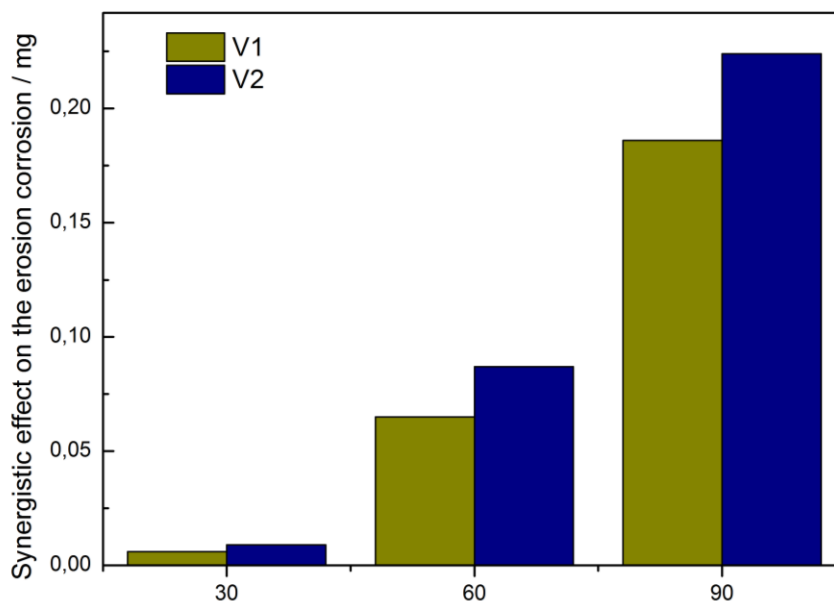
Figure 7. Mass loss for effect synergistic with erosive corrosive as function of velocity an angle.

In the figure 7, is obtained that the corrosive effect is the dominant mechanism of wear, follow by the synergism (erosion corrosion) and posterior the erosive, moreover it was observed that the electrochemical component benefits from dynamic environmental changes, even more of the impact action over the surface thus causes or not the hardening of it, since the impact to remove the outer layers of the material or, alternatively, to deform, increases the superficial area exposed and the capability of reaction to the surrounding medium, furthermore the agitation promotes the decreased of the electrolyte boundary layer on the material surface which leads a dominant mechanism of overstress by oxygen diffusion and ionic species onto the surface of the material. According to this dynamic, in a marine medium the erosive condition at 60° and 90° contributes to the highest electrochemical wear of the material. In the synergy mechanism of erosion corrosion, was shown the simultaneity in the processes: mechanical material removal by the erosion and the electrochemical corrosion process.

5. CONCLUSIONS

Observing the effect of erosion, it is evident that the erosion rate increases or decreases respectively in the same proportion with the increase or decrease of the angle of impact, independent of changes in fluid velocity. The potentiodynamics polarization curves obtained in the dynamic corrosion and erosion corrosion tests show that wear velocity increases when the impact angle and the fluid velocity increase. Furthermore, it was observed how is improved the behavior against the erosion corrosion with multilayers coating at 30° independent of the velocity, evidenced in the curves displacement towards lower values of current density with respect to angles of 60° and 90°. All the Tafel polarization curves indicate a general dissolution; this behavior is owing to the aggressive effect generated by the corrosion and the addition of erosion together. It is suggested to work coatings with a cathodic protection system at the angles of 60° and 90° in order that the coating does not affect corrosion in aggressive conditions

References

1. J. Olaya, S. Rodil, S. Muhl and E. Sánchez, *Thin Solid Films*, 474 (2005) 119.
2. F. Vacandio, Y. Massiani, P. Gravier and A. Garnier, *Surface and Coatings Technology*, 92 (1997) 221.
3. M. Pakala and R. Lin, *Surface and Coatings Technology*, 81 (1996) 233.
4. F. Medjani, R. Sanjinés, G. Allidi and A. Karimi, *Thin Solid Films*, 515 (2006) 260.
5. M. Penza, M. De Riccardis, L. Mirenghi, M. Tagliente and E. Verona, *Thin Solid Films*, 259 (1995) 154.
6. P. Hones, R. Sanjinés and F. Lévy, *Thin Solid Films*. 332 (1998) 240.
7. L. Cunha, M. Andritschky, L. Rebouta and R. Silva. *Thin Solid Films*, 317 (1998) 351.

8. G. Fuentes, R. Rodriguez, J.C. Avelar-Batista, J. Housden, F. Montalá, L.J. Carreras, A.B. Cristóbal, J.J. Damborenea and T.J. Tate, *Journal of Materials Processing Technology*, 167 (2005) 415.

9. H. Meng, X. Hu and A. Neville, *Wear*, 263 (2007) 355.

10. L. Niu and Y.F. Cheng, *Wear*, 265 (2008) 367.

11. J.L. Endrino, J.L. Fox-Rabinovich, and C. Gey, *Surface & Coatings Technology*, 200 (2006) 6840.

12. R.M. Soutoa, and H. Alanyalib, *Corrosion Science*, 42 (2000) 2201.

13. B.D. Jana and M.M. Stack, *Wear*, 259 (2005) 243.

14. D.E. Rosner, P. Talon, A.G. Konstandopoulos and M. Tassopoulos, *Prediction/correlation of particle deposition rates from polydispersed flowing suspensions and the nature/properties of resulting deposits,* Proc. Ist Int. Particle Technology Forum, AIChE, Denver, CO, (1994).

15. D.E. Rosner, P. Tandon and M.J. Labowsky, *AIChE JOURNAL*, 41 (1995) 1081.

16. Y.F. Khalil and D.E. Rosner, *Wear*, 201 (1996) 64.

17. J.G.A. Bitter, *Wear*, 6 (1963) 169.

18. M.S. Crowley, *Ceramic Bulletin*, 48 (1969) 707.

19. I. Finnie, *Wear*, 3 (1960) 87.

20. D.L. Keaims, W.C. Yang and W.G. Vaux, *Design of refractories for coal gasification and combustion systems*, EPRI AF-1151, Electric Power Research Institute, Pale Alto, CA, (1979).

21. ASTM G5 Standard Reference Test Method for Making Potentiostatic and Potentiodynamic Anodic Polarization Measurements, West Conshohocken, PA, American Society for Testing and Materials, 2003.

22. ASTM G59-04 Standard Test Method for Conducting Potentiodynamic Polarization Resistance Measurements, West Conshohocken, PA, American Society for Testing and Materials, 2004.

23. W. Aperador, C. Amaya and J. Bautista- Ruiz, *Rev. LatinAm. Metal. Mat,* 32 (2012) 210.

24. M. Fenker, M. Balzer, H.A. Jehn, H. Kappl, J.J Lee and Lee K-H, *Surf. Coat Tech*, 150 (2002) 101.

25. W. Aperador, J.C. Caicedo, C. España, G. Cabrera and C Amaya, *J Phys Chem Solids*, 71 (2010) 1754.

26. V.K. William, C- Barshilia-Harish, V. EzhilSelvi and K.S. Kalavati, Rajam, *Thin Solid Films*, 514 (2006) 204.

27. J.C. Caicedo, G. Cabrera, W. Aperador, H.H. Caicedo and A. Mejia, *Vacuum*, 86 (2012) 1886.